Current Research in Food Science 4 (2021) 414–420

Contents lists available at ScienceDirect

Current Research in Food Science

journal homepage: www.editorialmanager.com/crfs/

Rheo-NMR to investigate fat crystallization under shear

Ferre Rebry [a,1,*], Arnout Declerck [a,b,1], Karl-Friedrich Ratzsch [c,d], Manfred Wilhelm [c], Koen Dewettinck [b], Paul Van der Meeren [a]

[a] Particle and Interfacial Technology Group, Faculty of Bioscience Engineering, Ghent University, Coupure Links 653, B-9000 Ghent, Belgium
[b] Food Structure & Function Research Group, Faculty of Bioscience Engineering, Ghent University, Coupure Links 653, B-9000 Ghent, Belgium
[c] Institut für Technische Chemie und Polymerchemie, Karlsruhe Institute of Technology (KIT), D-76131 Karlsruhe, Germany
[d] Bruker Biospin GmbH, Rheinstetten, Germany

ARTICLE INFO

Keywords:
Rheo-NMR
Solid fat content
Crystal networks
Dynamic crystallization
Shear

ABSTRACT

It is well known that shear has an effect on fat crystallization. Whereas rheo-NMR has been used to study the impact of shear on the crystallization kinetics in the past, these methods mostly used a simple Teflon mixing shaft inside a sophisticated NMR instrument to apply shear to the sample. However, this method did not enable the determination of rheological parameters. In this work, a custom made low-field rheo-NMR device was evaluated, consisting of a commercial rheometer combined with a low-field permanent magnet to enable simultaneous rheological and NMR measurements. Two fats, i.e. partially hardened sunflower oil (PHSO) and soft palm mid fraction (sPMF), were submitted to several rheo-NMR experiments. The results of these experiments clearly indicated that these fats crystallized differently. First, PHSO crystallized faster than sPMF. Moreover, the latter seemed to crystallize in two steps. Initially a weak structure was formed when a low amount of solids was present, but this structure was replaced by a stronger network once more crystals were present. Both fats were studied under stagnant conditions, but also when submitted to low shear rates (1 s^{-1} and 5 s^{-1}). It was shown that the amount of solids necessary to obtain a viscosity of 10 Pa s was higher when the shear rate was higher. The strength of the formed crystal network at a given percentage of solids was also weaker as the shear rate during crystallization increased. Whereas these experiments were done non-isothermally, it was shown that rheo-NMR can also perfectly be used for isothermal measurements.

1. Introduction

Fat crystallization is a complex process. Due to the nature of the large amount of different triglycerides, crystallization happens over a range of temperatures and depending on the pre-treatment or process conditions, the formed fat crystals can be present in different polymorphic states and sizes.

Fat crystallization under shear has been studied by several authors. Mazzanti et al. (2003) studied crystal orientation and polymorphic transitions for different fats under shear by combining XRD and a Couette shear cell. This study showed that under shear, the crystals align to the shear direction and polymorphic transitions happen faster if higher shear rates are applied. Comparable results were found concerning the rate of the polymorphic transitions of cocoa butter (MacMillan and Roberts, 2002), milk fat (Mazzanti et al., 2009) and palm fat (Mazzanti et al., 2005). Moreover, cocoa butter crystallized under shear showed more mixed crystals, a faster crystallization and the formation of smaller crystals, yielding a stronger crystal network (Campos and Marangoni, 2014). However, other authors showed that the crystal network was weaker after shearing (Acevedo and Marangoni, 2013). Probably, a critical shear rate threshold exists as suggested by Patel and Dewettinck (2015).

The latter studies mostly focused on the polymorphic transitions in a fat under shear, whereas the influence of the amount of crystals or solid fat content (SFC) on the fat crystal network under shear is poorly studied. In the past, several rheo-NMR studies were already carried out. However, these studies focused on the NMR part, i.e. the SFC determination, but simplified the rheology part of the study. Mazzanti et al. (2008) applied a Teflon shaft inside a 10 mm internal diameter NMR tube in order to create a mini Couette cell at the bottom of the NMR tube. They studied the effect of shear on the SFC of canola stearin and canola oil mixtures, but found no difference between sheared and non-sheared samples. With

* Corresponding author.
E-mail address: ferre.rebry@ugent.be (F. Rebry).
[1] First author.

https://doi.org/10.1016/j.crfs.2021.05.004
Received 17 January 2021; Received in revised form 30 April 2021; Accepted 25 May 2021

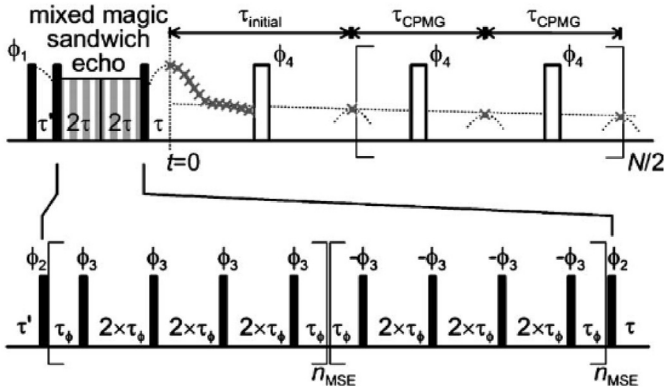

Fig. 1. Illustration of the magic sandwich echo sequence. 90° RF-pulses Φ_1, Φ_2, Φ_3 (indices show different phases); n_{MSE} number of repetitions of the 90° RF-pulse train; the different τ-values are waiting times between the different RF-pulses. Φ_4 are 180° RF-pulses (Maus et al., 2006).

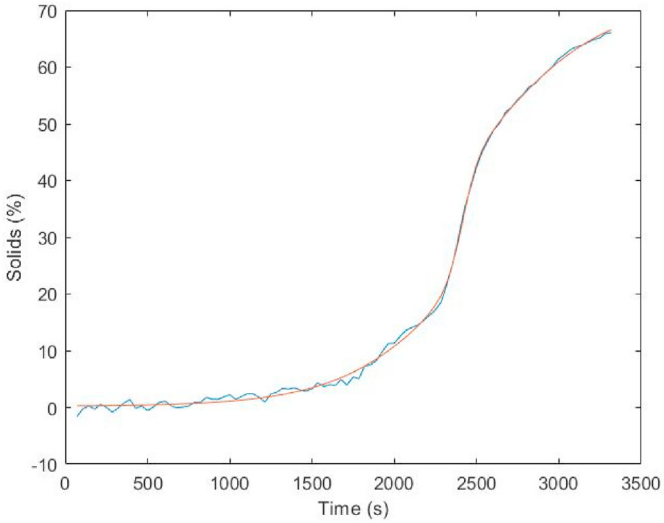

Fig. 2. Example of the double sigmoidal fit to the solids data as a function of time. The blue line represents the acquired data, while the red line represents the fit.

this set-up, the NMR FID signal and thus the SFC could be determined, but no rheological parameters (e.g. G′, G″) could be obtained. Mudge and Mazzanti (2009) showed that the SFC value of cocoa butter under shear did not only depend on the isothermal temperature, but also on the shear rate and the polymorphic state of the fat: at high shear rates (720 s^{-1}), the SFC was lower due to viscous heating of the sample.

Kaufmann et al. (2013) used a comparable set-up (a Teflon shaft combined with a laboratory mixer put into an NMR tube), but instead of following the SFC, they followed the polymorphic transition of milk fat/rapeseed oil mixtures. They used deconvolution methods to determine the decay rate of the FID signal, which is linked to the polymorphic state of the fat (Declerck et al., 2017). Rheo-NMR measurements were also done using high-resolution NMR. Gabriele et al. (2009) used diffusion NMR to estimate the globule size of dairy emulsions under shear.

The current work uses a recently developed and unique rheo-NMR set-up, which consists of a high-end rheometer with a custom made low-resolution time domain NMR set-up attached to it. Whereas this set-up was used before to investigate crystallization phenomena in plastics, we are not aware of any comparable study related to triglyceride crystallization. Hence, two different fats were selected, i.e. partially hardened sunflower oil (PHSO) and soft palm mid fraction (sPMF), which were submitted to both isothermal and non-isothermal rheo-NMR experiments to simultaneously determine the SFC as well as rheological parameters, such as the loss modulus (G″) and storage modulus (G').

2. Materials and methods

2.1. Studied fats

Partially hardened sunflower oil (PHSO) (SFC 5 °C: 73%; SFC 25 °C: 35%; 42% trans fatty acids) and soft palm mid fraction (sPMF) (SFC 5 °C: 71%; SFC 25 °C: 14%) were kindly supplied by Vandemoortele (Izegem, Belgium). The SFC values were determined via the f-factor method (AOCS Cd 16b-93).

2.2. Rheo-NMR

The rheo-NMR consisted out of an Ares G2 Rheometer (TA Instruments, New Castle, DE, USA) combined with a self-made 25 MHz NMR set-up. Further details about the set-up of the rheo-NMR can be found in the work of Ratzsch et al. (2017). During the oscillatory and rotational deformation experiments, the NMR data were collected every 32 s. A Magic Sandwich Echo (MSE) sequence (241 data points) was used, followed by a CPMG sequence (514 data points). As illustrated in Fig. 1, the MSE sequence consists out of multiple 90°-RF pulses separated by (two times) a waiting time τ_Φ which can be repeated multiple times (n_{MSE}) (Maus et al., 2006). The 90°-pulse length was 2.9 μs and the 180°-pulse length was 5.8 μs The n_{MSE} was equal to 1; τ_Φ, $\tau_{initial}$ and τ_{CPMG} were 150 μs. 16 scans per sample were used; per scan a relaxation delay of 2 s was used (resulting in 32 s per measurements). The receiver gain was fixed at 68 dB.

A parallel plate geometry with 13 mm diameter and 1 mm gap was used, consisting of ceramic plates, which do not interfere with the NMR measurements. The temperature of the sample was controlled using a heated (using a heating coil) or cooled (using a coil in an ice bath) N_2-flow at 1400 l/h. The latter set-up enabled a cooling rate of 1 °C/min. Before every measurement, the sample was kept at 65 °C for 5 min to melt all the crystals and was cooled as quickly as possible to 40 °C. At the latter temperature, the different measurements were started.

Three types of measurements were performed: a small oscillatory deformation temperature ramp experiment (acting as a no-shear experiment), a continuous rotational deformation experiment (at small shear rates in comparison with literature values of Acevedo and Marangoni, 2013; Mazzanti et al., 2003; Mazzanti et al., 2005; Mazzanti et al., 2008; Mudge and Mazzanti, 2009) followed by small amplitude oscillatory temperature ramp experiment and an isothermal oscillatory deformation experiment. During the small amplitude oscillatory experiment, a deformation of 0.005% and 0.00065% was applied on the sample at a frequency of 1 Hz. During these experiments, the temperature was lowered from 40 °C to 5 °C at a speed of 1 °C/min. The experiment was stopped when G' reached a final plateau value with no significant further change, meaning that the sample had nearly fully crystallized. The rotational deformation temperature ramp experiments started with applying a constant shear rate of 1 s^{-1} or 5 s^{-1} over the same temperature profile as discussed above. When a viscosity of 10 Pa s was obtained, the constant shear rate was stopped and a 0.005% oscillatory deformation was applied to characterize the crystal network. The isothermal measurements were performed at 23 °C; the sample was fast cooled to 23 °C and the oscillatory stress (0.005% deformation) was started at 23 ± 1 °C, which is close to the onset temperature of crystallization of PHSO.

2.3. Data processing

Matlab R2016b was used to process the obtained rheology and NMR data. As proposed by Räntzsch et al. (2018), the amount of solids was determined with Equation (1):

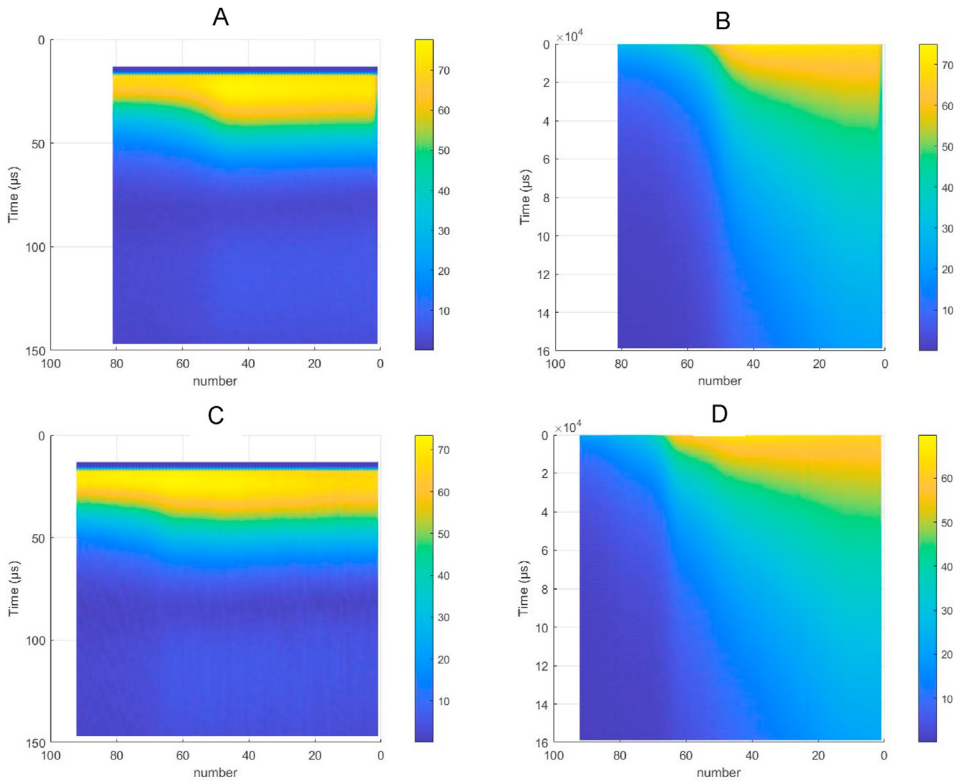

Fig. 3. MSE (A and C) and CPMG (B and D) profiles of PHSO (A and B) and sPMF (C and D) over the several measurements (indicated by the number on the X-axis) during cooling from 40 °C (first measurement: number = 1) to 5 °C (69th measurement), followed by an isothermal period at 5 °C (latest measurement). Blue refers to low intensities, yellow to high intensities. (For interpretation of the references to color in this figure legend, the reader is referred to the Web version of this article.)

$$Solids\ (\%) = \left(1 - \frac{I_{CPMG,0}}{I_{MSE,max}}\right)100 \quad (1)$$

$I_{CPMG,0}$ was determined by extrapolating the CPMG signal to t = 0 μs using an exponential function. This yields the overall signal intensity of the liquids. $I_{MSE,max}$ was determined by taking the highest value observed in the MSE results.

The rheology measurements had different time spacings than the NMR measurements. This was compensated by fitting a double sigmoidal curve to the obtained solids curve (i.e. amount of solids as a function of measuring time; Fig. 2). This analytical function was used to estimate the percentage of solids on the rheology time-scale, which enabled the creation of correlation figures between the storage modulus (G') or the viscosity and the amount of solids.

2.4. DSC

A TA Q1000 DSC with a refrigerated cooling system and an autosampler system (TA Instruments, New Castle, Delaware, USA) was used to determine the heat flow as a function of temperature (during cooling) and as a function of time (during the isothermal period). The device was calibrated using indium (TA Instruments), azobenzene (Sigma-Aldrich, Bornem, Belgium) and undecane (Acros Organics, Geel, Belgium). Nitrogen gas was used to purge the system. Samples (8–13 mg) were sealed hermitically in alodined aluminium pans (TA Instruments) and an empty pan was used as a reference. The temperature profile used resembled the temperature profile of the rheo-NMR. The samples were molten at 65 °C and kept at this temperature for 10 min, after which the samples were cooled fast (10 °C/min) to 40 °C. The samples were kept at 40 °C for 5 min and were further cooled to 5 °C at 1 °C/min. The samples were kept isothermally at 5 °C for 1 h. All samples were measured in triplicate.

3. Results and discussion

3.1. MSE-CPMG results

In Fig. 3, a contour plot of the MSE and CPMG profiles of PHSO and sPMF are shown under low oscillatory deformation (amplitude = 0.00065%). It has to be mentioned that an FID-CPMG sequence was tried as well. Due to the inhomogeneity of the magnetic field, the FID-signal fully decayed to an intensity of 0 within 50 μs at all measurement temperatures (i.e. 5–40 °C), and hence independent of the presence of crystals. It follows that the FID profile could not be used to extract information on the solid and liquid components within a fat blend. The MSE sequence (Maus et al., 2006) is a commonly used sequence in polymer research (Papon et al., 2011; Räntzsch et al., 2015; Weigand et al., 1994), but has not been used in fat research as a substitute for the FID sequence, as far as we know. The MSE sequence is used to refocus the signal of the crystalline phase (Maus et al., 2006). The echo of this signal is detected and thus there is no need to extrapolate the MSE signal using deconvolution techniques, which is required when trying to extract the amount of solids from the FID profile. This way, the MSE sequence avoids the problem concerning the dead time of the FID sequence. Furthermore, because the maximum intensity immediately after a 90° pulse can be detected and no extrapolation is necessary, the inhomogeneity of the magnetic field no longer poses an issue.

The CPMG intensities at short decay times show a clear gradient from high to low intensities (Fig. 2 B and 2 D) when the temperature got lower. As the CPMG signal is only determined by the liquid fraction, the latter indicates the creation of crystals. For the MSE signal, it was expected that the maximum intensity would remain constant because the MSE sequence determines the signal intensity of both solids and liquids. However, the maximum intensity was slightly variable (~10% difference

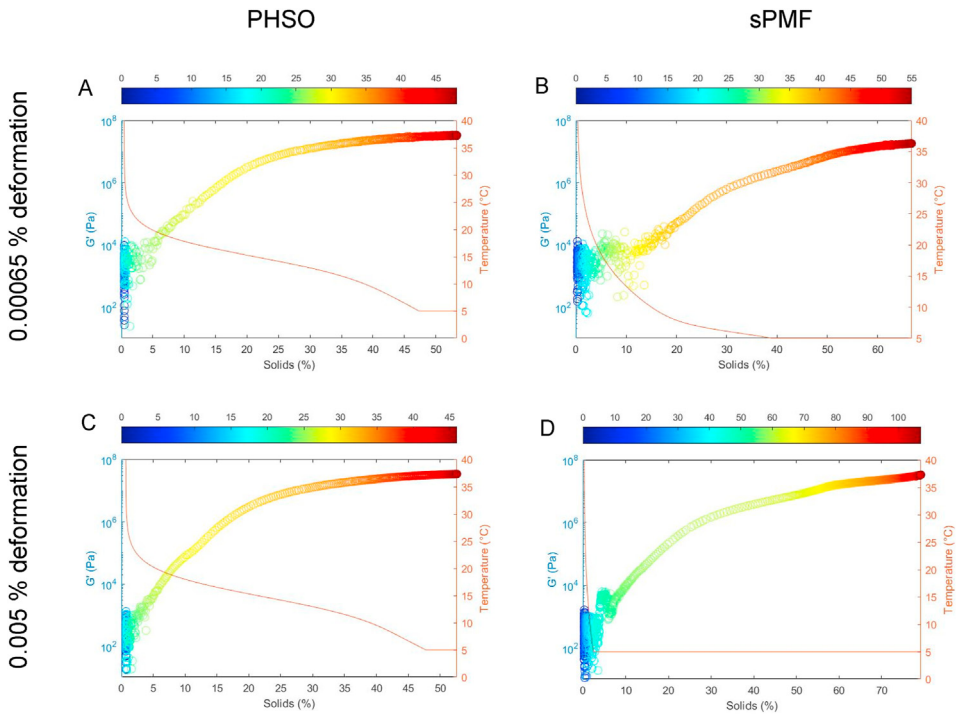

Fig. 4. Storage modulus (G′) as a function of the amount of solids during oscillation experiments with a deformation of either 0.00065% (A,B) or 0.005% (C,D) on PHSO (A,C) and sPMF (B,C). Color represents the measurement time in minutes and scales from dark blue at the start of the measurement to dark red at the end (A: 48, B: 55, C: 46 and D: 108 min). (For interpretation of the references to color in this figure legend, the reader is referred to the Web version of this article.)

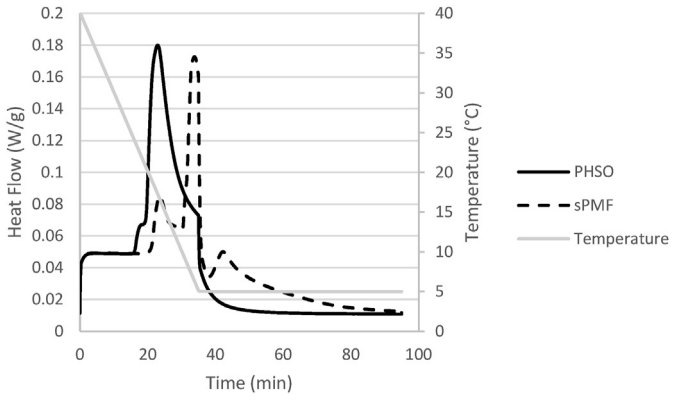

Fig. 5. Heat flow as a function of the time of PHSO and sPMF during cooling from 40 °C to 5 °C, followed by an isothermal period during 1 h at 5 °C.

between the highest and lowest maxima) for the different measurement numbers. A 3D plot of the MSE data of sPMF crystallization can be found in the supplementary data, showing an artifact at the start of the data collection. However, this artifact did not affect the peak intensity of the echo signal (Supplementary Fig. 1). Therefore the amount of solids could be deduced from the difference in intensity of the maximum MSE signal (which is the signal of the solid and liquid phase) and the extrapolated CPMG signal (which is the signal of the liquid phase).

3.2. Small oscillatory deformation

Fig. 4 shows that the elastic modulus (G′) rises during crystal formation for both PHSO and sPMF. The rheological parameters obtained at a deformation of 0.005% and 0.00065% (the lowest possible deformation) looked nearly identical, only the former showed lower noise. A clear rise in elastic modulus started when about 5% of solids was present in the case of PHSO. This means that the crystals at smaller solids fraction could be seen as individual, not-interconnected crystals. Starting from 5% of crystals onwards, the strength of the crystal network started to rapidly increase. It could be hypothesized that the formation of a crystal network might be correlated with the point where the liquid like behavior of the sample equals the solid like behavior, which corresponds to G' = G''. However, our data showed too much noise (G′ varying from 10^2 to 10^4 Pa s) at the start of the measurements to locate this point. From 50% solids onwards, a constant G′ slope was obtained and the experiment was stopped; under these conditions the G″ slope was also constant (data not shown). The G′ curve of sPMF was clearly distinct from the curve of PHSO: at about 5% of solids, a local maximum was found in the curves with 0.005% and 0.00065% deformation, respectively. Possibly, the initial crystals clumped together, whereas these clusters were later broken up into smaller clusters or recrystallized into a weaker structure. After this initial maximum, G' gradually rose to about 10^8 Pa, as was also the case with the PHSO.

The obtained DSC results of bulk PHSO (Fig. 5) showed two unresolved peaks: a minor peak at 19.3 min (20.7 °C) and a major peak at 23.5 min (16.5 °C). XRD measurements indicated an initial α-crystal peak, followed by a major β_1'-peak (Nelis et al., 2019). It has been shown that polymorphic transitions happen faster under shear (MacMillan and Roberts, 2002; Mazzanti et al. 2003, 2005, 2009). However, the shear exerted on the sample during small strain oscillatory deformation is expected to be too low to influence the polymorphic transitions. Hence, the initial solids are expected to be α-crystals, whereas the major rise in solids and G′ may be due to the formation of more firmly linked α- and β_1'-crystals. Once a temperature of 5 °C is reached, isothermal crystallization is hardly visible in the DSC results. In contrast, the rheo-NMR results clearly showed further crystallization even at the end of the rheo-NMR sequence (isothermal period), although less fast, as can be deduced from the fact that more data points are present around the same percentage of solids (Fig. 4). The DSC profile of sPMF displayed clearly separated peaks at 24.3 (15.7 °C), 34.3 (5.7 °C), and 43.4 min (5 °C). These clearly separated crystallization events might also be reflected in the rheo-NMR results, e.g. through the local maximum at low solids contents. XRD indicated that sPMF crystallization mainly involved

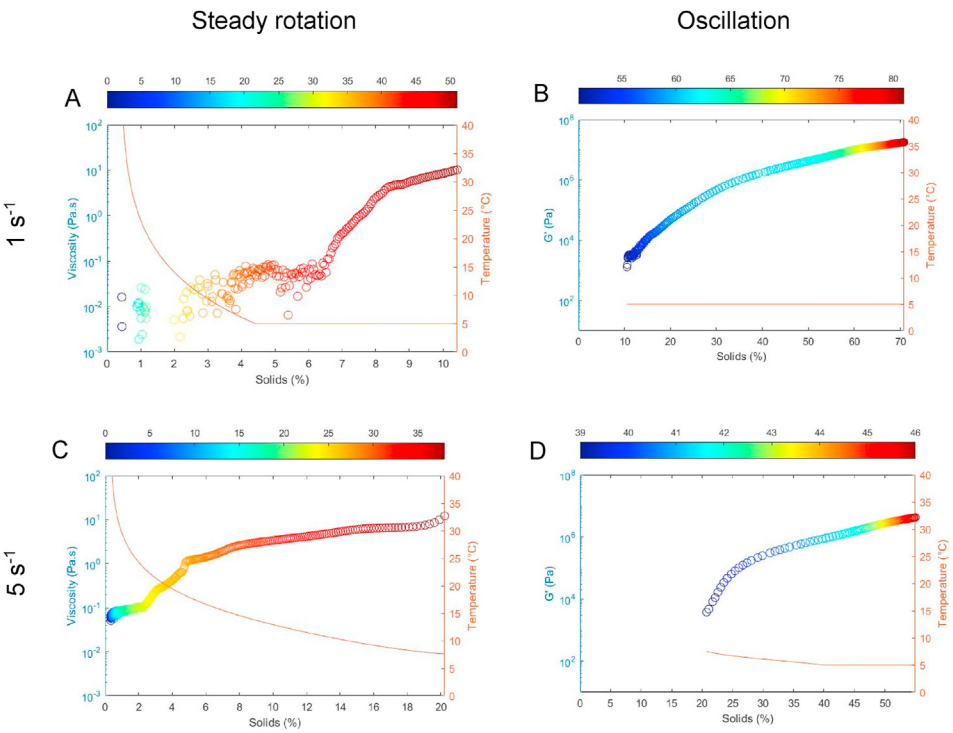

Fig. 6. Apparent viscosity at a shear rate of 1 s^{-1} (A) and 5 s^{-1} (C) and storage modulus at an oscillatory deformation of 0.005% (B, D) as a function of the amount of solids in sPMF. The color in the apparent viscosity curves ranges from dark blue at 0 min to dark red at 51 (A) or 38 min (C), whereas the color in the G′-curves starts at dark blue at the end of the rotation experiment and extends to dark red at 81 min (B) or 46 min (D). (For interpretation of the references to color in this figure legend, the reader is referred to the Web version of this article.)

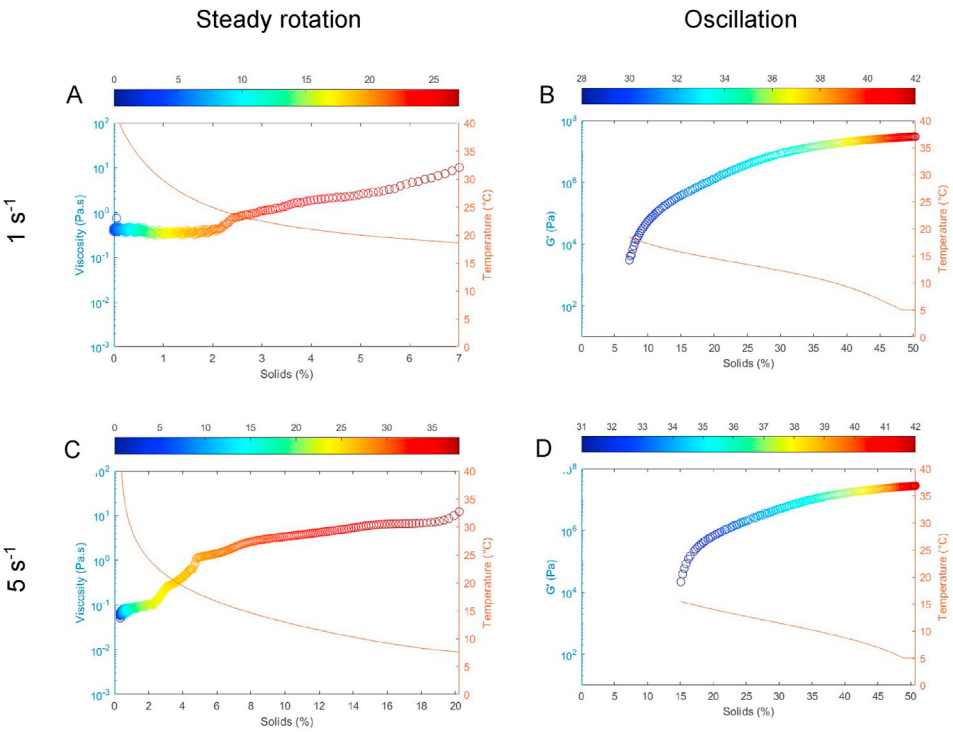

Fig. 7. Apparent viscosity at a shear rate of 1 s^{-1} (A) and 5 s^{-1} (B) and subsequent storage modulus at an oscillatory deformation of 0.005% (C, D), as a function of the amount of solids in PHSO. The color in the viscosity curve starts at dark blue at 0 min to dark red at 28 and 31 min for 1 s^{-1} and 5 s^{-1}, respectively. The color in the G′-curve starts at dark blue at the end time of the rotation experiment to dark red at 50 and 42 min for 1 s^{-1} and 5 s^{-1}, respectively. (For interpretation of the references to color in this figure legend, the reader is referred to the Web version of this article.)

α-crystals (Nelis et al., 2019).

Note that the small deviation from 0% solids at 40 °C is caused by the polynomial curve that was fit to the calculated solids data. The actual data shows a slight variability (±1%) around the 0% solids mark at the start of the measurement, while the polynomial fit slightly increases in this timeframe (Supplementary Fig. 2).

The calculated percentage of solids at the end of the experiment (at 5 °C) shows a good correlation with the SFC for both PHSO and sPMF. Nelis et al. (2019) published SFC results of isothermal crystallization at 5 °C showing ± 62% solids after 50 min and ±80% solids after 100 min for PHSO and sPMF, respectively. Our values are comparable to the SFC value of sPMF at 5 °C as determined by the AOCS-approved method, but lower for PHSO. This is, however, not unexpected as another sample processing was used: whereas a gradual cooling was applied in rheo-NMR, the OACS-approved SFC determination started by incubation at 0 °C, followed by subsequent incubation at 5 °C.

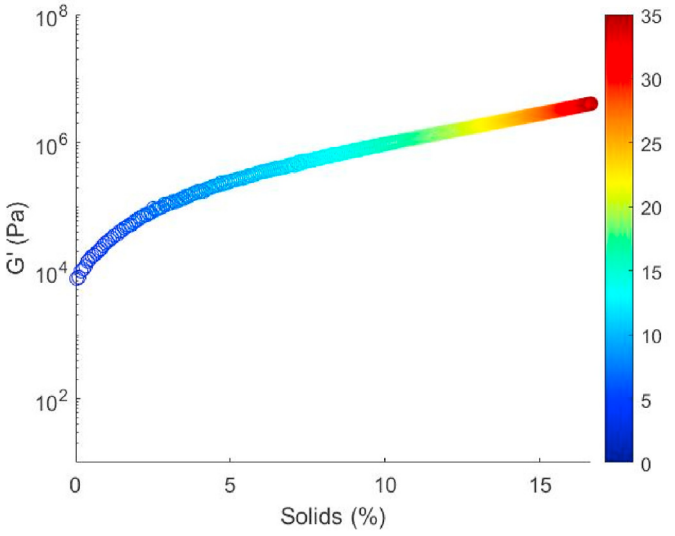

Fig. 8. Storage modulus of PHSO as a function of the amount of solids during isothermal crystallization at 23 °C. The color scales from dark blue at 0 min to dark red at 35 min. (For interpretation of the references to color in this figure legend, the reader is referred to the Web version of this article.)

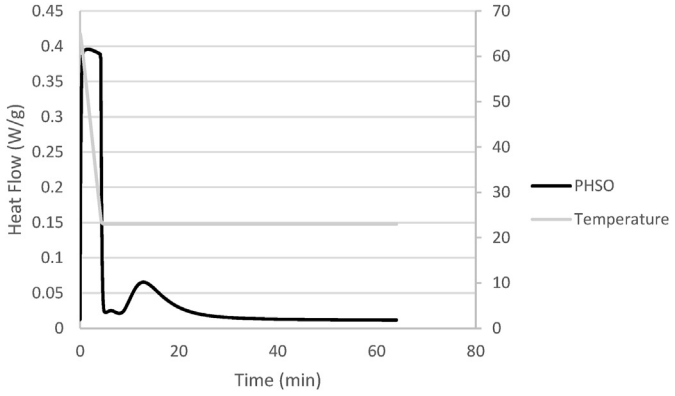

Fig. 9. Heat flow as a function of time of PHSO after fast cooling (10 °C/min) from 60 °C to 23 °C, followed by an isothermal period at 23 °C of 1 h.

3.3. Small rotational deformation followed by oscillatory deformation

When a small constant shear rate was applied to sPMF (Fig. 6), the viscosity of the sample initially remained between 10^{-2} and 10^{-1} Pa s. Starting from 7% of solids, a rise in viscosity was visible and at 10% of solids the viscosity already reached 10 Pas, showing that even a small amount of solids can produce a strong crystal network. The subsequent oscillation measurements showed an increase in G' when the amount of solids rose, which was also observed in the small deformation oscillatory experiments in Fig. 4. With an increase in shear rate, the amount of solids or crystals necessary to obtain a viscosity of 10 Pas increased to 20%.

In comparison with sPMF, the PHSO sample already started rising in viscosity when 1–2% of crystals were present (Fig. 7). When the shear rate was 1 s^{-1}, 10 Pas was obtained with an amount of solids of 7%, while at a higher shear rate of 5 s^{-1}, the limit of 10 Pas was only obtained at 15% of solids. Hence, a higher shear rate made it more difficult to make a strong network. The results of the oscillation measurements did not differ: in both cases, a clear increase in G' as a function of the amount of solids was found.

When comparing the speed of crystallization and crystal network formation of PHSO and sPMF, both occurred faster in PHSO than in sPMF. This is related to the triacyclglycerol composition of both fats. Hydrogenated fats containing trans fatty acids are known to crystallize faster than their nonhydrogenated counterparts (De Graef et al., 2007). Again, the MSE sequence seemed to provide appropriate results for the percentage of solids. Nelis et al. (2019) published isothermal crystallization SFC results at 5 °C showing ± 76% solids after 60 min for sPMF.

3.4. Isothermal crystallization

At 23 °C, which is close to the onset temperature of crystallization of PHSO (23.96 ± 0.07 °C), the heat flow (Fig. 9), as well as the amount of solids and G' were measured (Fig. 8). The DSC results (Fig. 9) show that PHSO crystallized at 23 °C, as seen from the obvious peak in the isothermal DSC profile. The rheo-NMR results of PHSO were in line with the DSC results: upon holding at 23 °C, an increasing amount of crystals were formed (up to 16% within the observation window). Comparing the estimated solids fraction with the experimentally determined SFC at 25 °C (i.e. 35 %), a lower value is obtained. This underestimation is a logical consequence of the different sample pretreatment: whereas the solids fraction was determined after cooling rapidly from 60 to 23 °C, the SFC is determined by crystallization at 0 °C, followed by partial melting at 25 °C. Fig. 8 also nicely illustrates that a crystal network was created as seen from the 1000-fold increase in elastic modulus. This was observed immediately at the start of the measurements (blue dots in Fig. 8), as was the case with the DSC analysis. As the deformation was only 0.005%, no influence on the crystallization was expected. Comparing Figs. 8–7 C and D and Fig. 4 A and C, it is clear that a lower applied shear (or the absence thereof) during crystallization resulted in a stronger crystal network at a lower percentage of solids. Thus, an elastic modulus of 10^5 Pa was reached for PHSO at 17 and 12% solids when the crystallization was initiated at a shear rate of 5 and 1 s^{-1}, resp. At a shear of 0 s^{-1}, 10^5 Pa was reached at 10% solids in Fig. 4 A and C, and at only 2% of solids in Fig. 8. This indicates that a fast cooling results in a stronger crystal network at the same percentage of solids, which is likely due to the formation of a larger amount of smaller fat crystals (Wiking et al., 2009).

4. Conclusion

Rheo-NMR has been shown to be a very promising technique to study fat crystallization under shear. The used device focused strongly on the rheological part of the rheo-NMR combination, with a simplified NMR extension. Whereas the magnetic field inhomogeneity did not enable SFC determination by FID signal analysis, the MSE sequence yielded reliable measurements of the percentage of solids. The technique enabled to mimic industrial process conditions, which often take place under shear. Moreover, it allowed to determine the correlation between changes in the elastic modulus and in the degree of crystallinity. The results of rheo-NMR measurements on PHSO and sPMF showed that the fat network creation of both fats differed notably. Moreover, valuable insights on the effect of shear during crystallization were gained: when shear was applied during the initial crystallization steps, a smaller shear rate resulted in a stronger crystal network at a lower percentage of solids for both sPMF and PHSO.

CRediT authorship contribution statement

Ferre Rebry: Conceptualization, Writing – original draft, Data curation, Software, Writing- Reviewing and Editing. **Arnout Declerck:** Conceptualization, Writing – original draft, Data curation, Software, experimental work, Methodology. **Karl-Friedrich Ratzsch:** Writing-Reviewing and Editing, Supervision. **Manfred Wilhelm:** Writing-Reviewing and Editing, Supervision. **Koen Dewettinck:** Writing-Reviewing and Editing. **Paul Van der Meeren:** Conceptualization, Writing- Reviewing and Editing, Supervision, Methodology.

Declaration of competing interest

The authors declare the following financial interests/personal relationships which may be considered as potential competing interests: The Rheo-NMR setup is now being further developed at Bruker BioSpin GmbH, current employer of co-author Karl-Friedrich Ratzsch.

Acknowledgements

We would like to thank Begüm Ozen to receive us at the Karlsruher Institut für Technologie and for her assistance with the rheo-NMR experiments. Funding: This work was supported by the Special Research Fund (BOF) (Grant number: BOF15/24j/086).

Appendix A. Supplementary data

Supplementary data to this article can be found online at https://doi.org/10.1016/j.crfs.2021.05.004.

References

Acevedo, N.C., Marangoni, A.G., 20132013. Functionalization of non-interesterified mixtures of fully hydrogenated fats using shear processing. Food Bioprocess Technol. 7 (2), 575–587.

Campos, R., Marangoni, A.G., 2014. Crystallization dynamics of shear worked cocoa butter. Cryst. Growth Des. 14, 1199–1210.

Declerck, A., Nelis, V., Rimaux, T., Dewettinck, K., Van der Meeren, P., 2017. Influence of polymorphism on the solid fat content determined by FID deconvolution. Eur. J. Lipid Sci. Technol. 120, 1–27.

De Graef, V., Foubert, I., Smith, K.W., Cain, F.W., Dewettinck, K., 2007. Crystallization behaviour and texture of trans-containing and trans-free palm oil based confectionery fats. J. Agric. Food Chem. 55, 10258–10265.

Kaufmann, N., Kirkensgaard, J.J.K., Andersen, U., Wiking, L., 2013. Shear and rapeseed oil addition affect the crystal polymorphic behaviour of milk fat. J. Am. Oil Chem. Soc. 90, 871–880.

MacMillan, S.D., Roberts, K.J., 2002. In situ small angle X-ray scattering (SAXS) studies of polymorphism with the associated crystallization of cocoa butter fat using shearing conditions. Cryst. Growth Des. 2 (3), 221–226.

Maus, A., Hertlein, C., Saalwächter, K., 2006. A robust proton NMR method to investigate hard/soft ratios, crystallinity and component mobility in polymers. Macromol. Chem. Phys. 207, 1150–1158.

Mazzanti, G., Guthrie, S.E., Sirota, E.B., Marangoni, A.G., 2003. Orientation and phase transitions of fat crystals under shear. Cryst. Growth Des. 3 (5), 721–725.

Mazzanti, G., Marangoni, A.G., Idziak, S.H.J., 2005. Modeling phase transitions during the crystallization of a multicomponent fat under shear. Phys. Rev. 71, 041607.

Mazzanti, G., Marangoni, A.G., Idziak, S.H.J., 2009. Synchrotron study on crystallization kinetics of milk fat under shear flow. Food Res. Int. 42 (5–6), 682–694.

Mazzanti, G., Mudge, E.M., Anom, E.Y., 2008. In situ rheo-NMR measurements of solid fat content. J. Am. Oil Chem. Soc. 85, 405–412.

Mudge, E.M., Mazzanti, G., 2009. Rheo-NMR measurements of cocoa butter crystallized under shear flow. Cryst. Growth Des. 9 (7), 3111–3118.

Nelis, V., Declerck, A., De Neve, L., Moens, K., Dewettinck, K., Van der Meeren, P., 2019. Fat crystallization and melting in W/O/W double emulsions: comparison between bulk and emulsified state. Colloid. Surface. Physicochem. Eng. Aspect. 566, 196–206.

Patel, A.R., Dewettinck, K., 2015. Current update on the influence of minor lipid components, shear and presence of interfaces on fat crystallization. Curr. Opin. Food Sci. 3, 65–70.

Räntzsch, V., Haas, M., Özen, M.B., Ratzsch, K.F., Riazi, K., Kauffmann-Weiss, S., Palacios, J.K., Müller, A.J., Vittorias, I., Guthausen, G., Wilhelm, M., 2018. Polymer crystallinity and crystallization kinetics via benchtop 1H NMR relaxometry: revisited method, data analysis and experiments on common polymers. Polymer 145 (6), 162–173.

Räntzsch, V., Ratzsch, K.F., Guthausen, G., Schlabach, S., Wilhelm, M., 2015. Molecular dynamics of polymer composites using rheology and combined rheoNMR on the example of TiO_2-filled poly(n-alkyl methacrylates) and trans-1,4-polyisoprene. Soft Mater. 12, S4–S13.

Ratzsch, K.F., Friedrich, C., Wilhelm, M., 2017. Low-field rheo-NMR: a novel combination of NMR relaxometry with high end shear rheology. J. Rheol. 61 (5), 905–917.

Weigand, F., Fülber, C., Blümich, B., Spiess, H.W., 1994. Spatially resolved NMR of rigid polymers and elastomers. Magn. Reson. Imag. 12 (2), 301–304.

Wiking, L., De Graef, V., Rasmussen, M., Dewettinck, K., 2009. Relations between crystallisation mechanisms and microstructure of milk fat. Int. Dairy J. 19, 424–430.